

Study on Stabilization of Vertical Position of Tokamak Plasma with Local Helical Coils in TOKASTAR-2

Kouhei YASUDA, Takaaki FUJITA, Atsushi OKAMOTO, Hideki ARIMOTO, Ryohei IKEDA, Sora KIMATA and Keitaro KADO

Graduate School of Engineering, Nagoya University, Furo-sho, Chikusa-ku, Nagoya 464-8603, Japan

(Received 2 June 2020 / Accepted 11 October 2020)

We investigated effects of the local helical magnetic field on the plasma vertical position to suppress Vertical Displacement Event (VDE) in TOKASTAR-2. Conditions for VDE occurrence were investigated on the vertical plasma position and the current of coils for elongating the plasma, with and without the helical field, and no clear effects of the helical field were observed. Even though the helical coil currents were increased and the plasma vertical position were adjusted, the existing local helical coils were not effective to stabilize the plasma vertical position, resulting in the plasma current quench. We evaluated the effective radial field, which is expected to stabilize the plasma vertical position, using magnetic field line trace calculation. We found that the distribution and magnitude of the effective radial field generated by the existing helical coils were not appropriate for stabilization of the plasma vertical position. We designed new local helical coils consisting of triangular coils located on the upper and lower sides of the plasma. The new coils can generate the effective radial magnetic field, which is expected to stabilize the plasma vertical position.

© 2020 The Japan Society of Plasma Science and Nuclear Fusion Research

Keywords: helical field application, VDE, local helical coil

DOI: 10.1585/pfr.15.1402083

1. Introduction

Elongated plasmas are suitable for achieving the high beta values and good confinement in tokamaks but suffer from vertical positional instabilities leading to Vertical Displacement Event (VDE). In general, plasma vertical positions are controlled by shell effects of the conducting walls near the plasma and active feedback systems using axisymmetric coils. On the other hand, helical magnetic field is thought to provide improved positional stabilities. The stabilization of the plasma positions by applying the helical field to the tokamak plasmas has been shown in some devices [1–3]. For example, stabilization of the plasma vertical position with the high plasma elongation ($\kappa \sim 2$) using a continuously-wound helical coil was shown in Ref. [3].

TOKASTAR-2 is a tokamak-helical hybrid device with local helical magnetic field coils. One of the main objectives is stabilization of the plasma position using the local helical coils. The shape and arrangement of the helical coils are simple; they are divided to outside helical coils and upper and lower helical coils. It is easier to install local helical coils in tokamak devices than continuously-wound helical coils. Figure 1 shows the coil systems of TOKASTAR-2. The tokamak and helical coil systems can be operated independently or simultaneously. The helical coil system consists of two HF (Helical Field) coils in parallelogram shape, four AHF (Additional Helical Field)

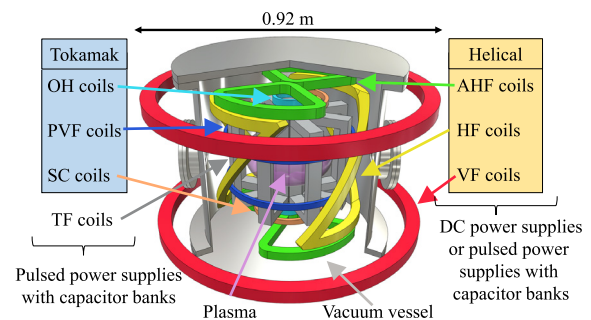


Fig. 1 Coil systems of TOKASTAR-2.

coils in fan shape and two circular VF (Vertical Field) coils. The HF coils are located on the low-field side while the AHF coils are mounted on upper and lower sides of the plasma. They were designed so that the closed magnetic surfaces are generated without the plasma current. The tokamak coil system consists of three-block OH (Ohmic Heating) coils and two PVF (Pulse Vertical Field) coils and two SC (Shape Control) coils. The PVF coils are located on the low-field side and used to generate a varying vertical field for the tokamak equilibrium. The SC coils are located on the upper and lower sides of the plasma to vary the plasma elongation and study the vertical stability of elongated plasmas. The SC coils were installed in the Spring of 2016 while the power supply for them was completed by the Summer of 2018. Eight TF (Toroidal Field) coils

author's e-mail: yasuda.kouhei@g.mbox.nagoya-u.ac.jp

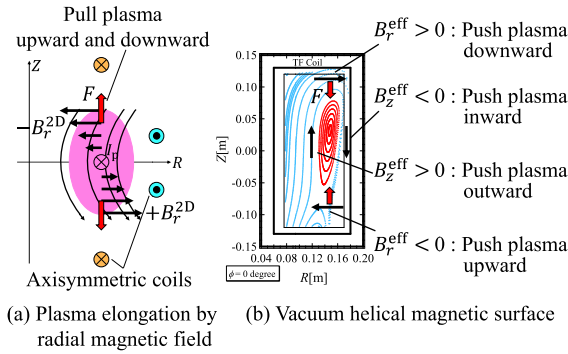


Fig. 2 Stabilization of the tokamak plasma position by applying the helical field.

are used to generate a toroidal field. The VF coils are connected to DC power supplies and the others are connected to pulsed power supplies with capacitor banks in this study.

Figure 2 (a) shows elongated tokamak equilibrium and principle of vertical positional instability. Upper and lower axisymmetric coils generate radial magnetic field whose direction is reversed at the equatorial plane in order to elongate the plasma. The radial field pulls the plasma and destabilizes the plasma vertical position. Figure 2 (b) shows the helical vacuum magnetic surface and the stabilization of the tokamak plasma position by applying the helical field conceptually. The rotational transform of the helical field generates the effective axisymmetric poloidal field $B_{r,z}^{eff}$. The effective radial magnetic field, whose direction is reversed at the equatorial plane, acts as restoring force, which is expected to stabilize the plasma vertical position [4]. In other words, this effective radial field can cancel the radial field generated by the axisymmetric coils, which destabilizes the plasma vertical position. Moreover, the effective vertical field can stabilize the plasma horizontal position.

The effect of the helical field application on the plasma horizontal position was observed with magnetic field measurements [5, 6] and with a high-speed camera [7] in TOKASTAR-2. In this paper, we investigate effects of the helical field application on the plasma vertical position to suppress VDEs.

2. Experiments

To study the effect of the helical field, the local helical field was applied on the tokamak plasmas. No feedback control system for the plasma position was used and the coil currents were pre-programmed with the power supplies with capacitor banks or DC power supplies. In this study, HF coils and AHF coils were connected in series. The number of turns of the HF coils and the AHF coils are 98 turns and 126 turns respectively and then the ratio of the coil currents (Aturns) between the AHF coils and the HF coils is $126/98 \sim 1.286$. The upper or lower VF coil was used to generate the radial, not vertical, field to

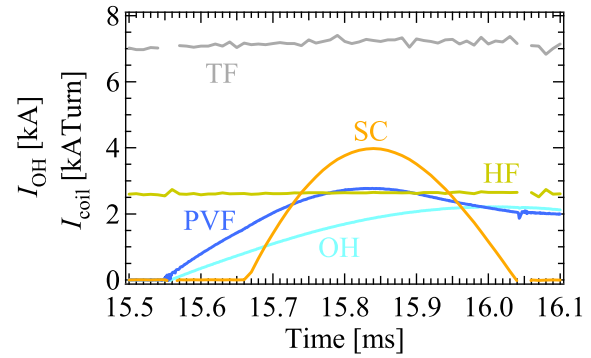


Fig. 3 A typical waveform of the coil currents.

adjust the plasma vertical position slightly. The upper VF coil was used to move the plasma vertical position upward, while the lower VF coil was used to move it downward. The time constants of the helical coil current and the TF coil current are much larger than those of the PVF coils, OH coils and SC coils. Figure 3 shows a typical waveform of those coil currents. In this case, the peak SC coil current of ~ 4 kAturns was obtained for the charging voltage of the SC coils of 0.28 kV. The sequence is as follows. (1) Stationary VF coil current starts to rise at the end of charging the capacitor banks, (2) The helical coil current and TF coil current start to rise, (3) An RF wave (2.45 GHz) is injected for the pre-ionization with electron cyclotron resonance heating (ECRH). (4) The OH coil current and PVF coil current start to rise to drive the plasma current at the flat top of the helical coil current and the TF coil current. The helical coil current and TF coil current are quasi-stationary during the plasma discharges. (5) The SC coil current start to rise to increase the plasma elongation. In this study, nitrogen was used as the working gas. We scanned the charging voltages of capacitor banks for the PVF coils (V_{PVF}), the SC coils (V_{SC}), the helical (HF and AHF) coils ($V_{Helical}$) and the VF coil current (I_{VF}) to adjust the plasma horizontal position, the plasma elongation, the magnitude of the helical field and the plasma vertical position, respectively. The plasma position and shape were estimated by the filament method based on external magnetic measurements [6]. In this paper, the plasma horizontal and vertical position are evaluated as the position of the current centroid obtained by the filament method. The position and shape of the tokamak plasmas with the helical field were obtained ignoring the three-dimensionality of the plasma current distribution, using the fields measured with probes located at a single toroidal location, together with flux loops. We confirmed the validity of the filament method by comparing the plasma positions obtained by it with images measured with a high-speed camera. The results of the filament method were in good agreement with the camera-image when the helical coil current was small, for example the HF coil current was 2.6 kAturns, while the difference of the results between the filament method and

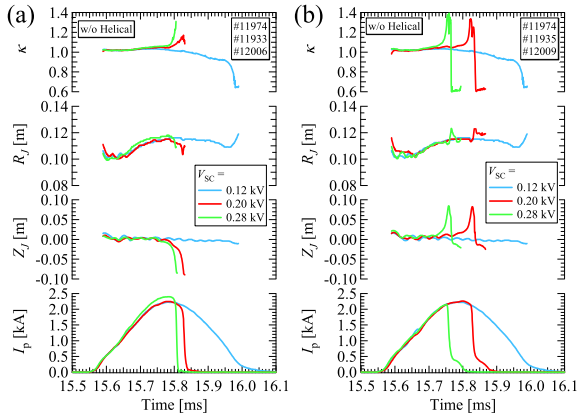


Fig. 4 Time evolution of the plasma current I_p , the plasma horizontal R_J and vertical Z_J positions and the elongation κ for three values of V_{SC} with (a) downward VDEs and (b) upward VDEs in the case without the helical field.

the camera-image became larger as the helical coil current was increased.

We investigated the dependence of the vertical stability and the plasma elongation on the magnitude of the magnetic field generated by the SC coils. Figure 4 shows time evolution of the plasma current I_p , the plasma horizontal position R_J , the vertical position Z_J and the elongation κ for three values of V_{SC} ($= 0.12, 0.20, 0.28$ kV) without the helical field. We selected the appropriate plasma discharges with almost the same plasma positions in each V_{SC} from discharges obtained by changing the current of the PVF coils and the VF coils. Figures 4(a) and (b) show the plasma discharges with downward VDE and upward VDE, respectively. In Fig. 4(a) we moved the plasma vertical position downward slightly, while in Fig. 4(b) we moved it upward slightly. The vertical position was stable when the V_{SC} was small (0.12 kV), while VDEs were caused by the vertical positional instability when V_{SC} was increased (0.20, 0.28 kV). Plasma current quenches were also observed. In upward-VDE discharges, moving back to the equatorial plane after VDEs was observed. This phenomenon was observed in downward VDEs when we reversed the direction of the toroidal field, and thus we consider this is caused by the error field of the TF coils. Figure 5(a) shows the vertical position as a function of the elongation of the plasma discharge in Fig. 4(a) with $V_{SC} = 0.28$ kV. The plasma was almost at the equatorial plane while the elongation increased gradually to ~ 1.05 . The VDE occurred after the elongation increased to ~ 1.05 , and then the elongation increased rapidly during the VDE. Figure 5(b) shows an enlarged view of the plasma vertical position and the plasma current of the same discharge. As shown in Fig. 5(b), the plasma current quench occurred after the VDE, typically when the plasma vertical displacement from the equatorial plane exceeded 0.04 m. The plasma current quench rate was higher than 100 MA/s.

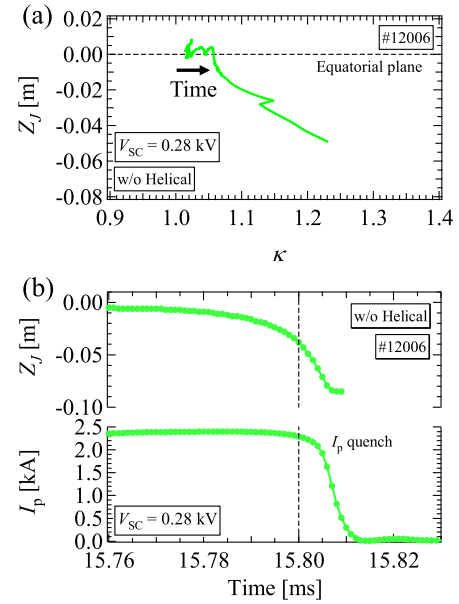


Fig. 5 (a) The vertical position as a function of the elongation and (b) the enlarged view of Fig. 4 (a) for $V_{SC} = 0.28$ kV.

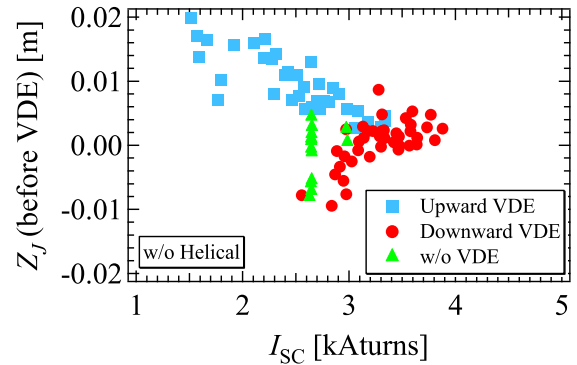


Fig. 6 The plasma vertical position before VDEs as a function of the SC coil current, I_{SC} , in the case without the helical field. The blue, red and green symbols denote plasma discharges with upward VDEs, downward VDEs and no VDEs, respectively.

Figure 6 shows the plasma vertical position before VDEs as a function of the SC coil current, I_{SC} , in the case without the helical field. The vertical axis is the plasma vertical positions evaluated by averaging the vertical positions from the start-up of the discharges until the VDE occurrence. We defined the time when the VDEs occurred as the time when the plasma vertical positions move by ± 0.01 m from the averaged vertical positions. The five values of V_{SC} ($= 0.12, 0.16, 0.20, 0.24, 0.28$ kV) were used. The SC coil currents were evaluated as the values when the VDEs occurred in discharges with VDE while as the maximum values in discharges without VDE. The direction of VDEs depends on the plasma vertical position before VDEs. Upward VDEs occurred when the plasma vertical

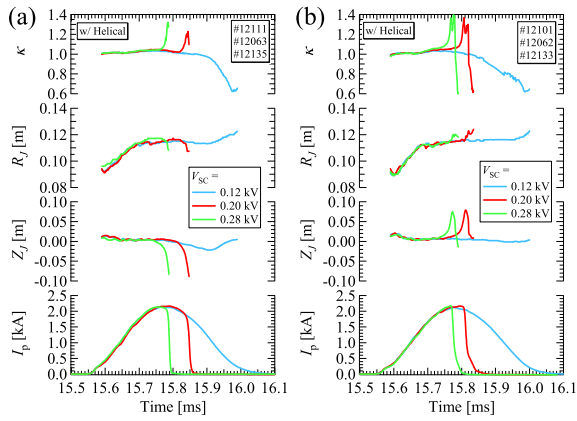


Fig. 7 Time evolution of the plasma current I_p , the plasma horizontal R_J and vertical Z_J positions and the elongation κ for three values of V_{SC} with (a) downward VDEs and (b) upward VDEs in the case with the helical field. The HF coil current was ~ 2.6 kAturns.

position was above the equatorial plane, while downward VDEs occurred when the plasma vertical position was below it. In the case with small I_{SC} (~ 2.6 kAturns), no VDEs occurred when the plasma vertical position was close to the equatorial plane, while VDEs occurred when it was far from the equatorial plane. On the other hand, in the case with large I_{SC} (> 3 kAturns), VDEs occurred even when the plasma vertical position was close to the equatorial plane.

Next, we investigated the effect of the helical magnetic field on the plasma vertical positions by applying it on the tokamak plasmas. Figure 7 shows time evolution of the plasma current, the plasma horizontal and vertical positions and the elongation for three values of V_{SC} ($= 0.12, 0.20, 0.28$ kV) with the helical field. The HF coil current I_{HF} was ~ 2.6 kAturns. The same as the case without the helical field, Fig. 4, the vertical position was stable when the V_{SC} was small, while VDEs were caused when V_{SC} was increased. We tried to stabilize the plasma vertical position with the stronger helical magnetic field, and we increased the charging voltage of the capacitor banks for the helical coils. Figure 8 shows the plasma vertical position Z_J before VDEs as a function of the maximum of plasma current in each strength of the helical magnetic field for a low value of V_{SC} ($= 0.12$ kV). The I_{HF} was 0 kAturns (without the helical field), ~ 2.6 kAturns, ~ 5.2 kAturns and ~ 7.8 kAturns. When I_{HF} was ~ 2.6 kAturns, downward VDEs were observed at $Z_J \sim 0$ m, as shown by open red circles, where no VDEs were observed when I_{HF} was 0 kAturns. VDEs occurred in all discharges in the case with stronger helical fields, $I_{HF} \sim 5.2$ kAturns and ~ 7.8 kAturns. Moreover, the achievable maximum of the plasma current decreased with the strength of the helical field. The stabilization of the plasma vertical position was not observed even with small V_{SC} and strong helical fields. From these experiments, we

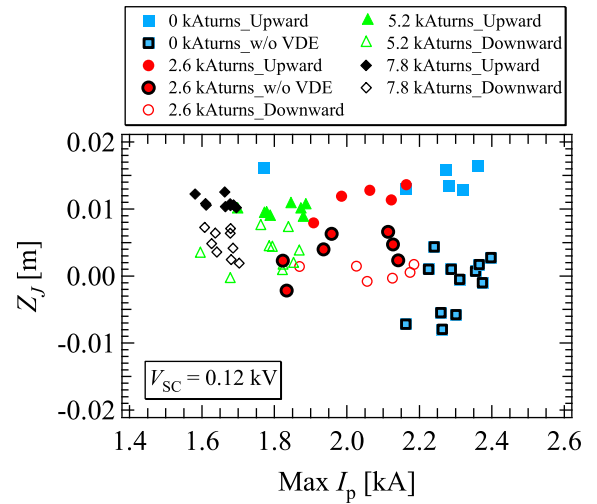


Fig. 8 The plasma vertical position before VDEs as a function of the maximum of plasma current in each strength of the helical magnetic field for $V_{SC} = 0.12$ kV. The values in the legend are the HF coil current, I_{HF} . The closed symbols, the open symbols and the closed symbols with black frames denote plasma discharges with upward VDEs, downward VDEs and no VDEs, respectively.

concluded that the existing helical coils are not effective to stabilize the plasma vertical position.

3. Design of New Local Helical Coils

To investigate the reason why the existing helical coils were not effective to stabilize the plasma vertical positions, we evaluated the effective radial magnetic field B_r^{eff} generated by the helical coils, as described in Sec. 1. We evaluated it using magnetic field line trace calculation. In this study, we defined B_r^{eff} as average of the radial field along the magnetic field line for 2π of the toroidal angle ϕ expressed as

$$B_r^{\text{eff}} = \int_{\phi=0}^{2\pi} B_r ds \Big/ \int_{\phi=0}^{2\pi} ds, \quad (1)$$

where ds is small arc length along a magnetic field line. Figure 9 shows an example of projection on the poloidal plane of the magnetic field line generated by helical coils from toroidal angle 0 to 2π . In this case, the magnetic field line drifts outward in the radial direction after going around the toroidal direction. Thus, it is expected that this helical magnetic field line acts as outward radial field, $B_r^{\text{eff}} > 0$, effectively. The calculation point (R_{av}, Z_{av}) was defined as the average of the position along the integration path. Each coil was approximated as a single filament in the magnetic field line calculations.

Figure 10 shows the radial fields generated by the existing helical coils and axisymmetric coils as a function of the vertical coordinate Z at $R = 0.12$ m, which is the center of the plasma production region. The effective radial field by the existing helical coils are calculated with the currents

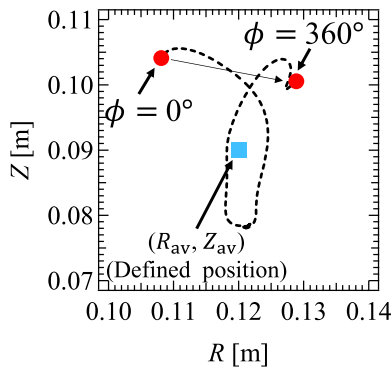


Fig. 9 An Example of the helical magnetic field line.

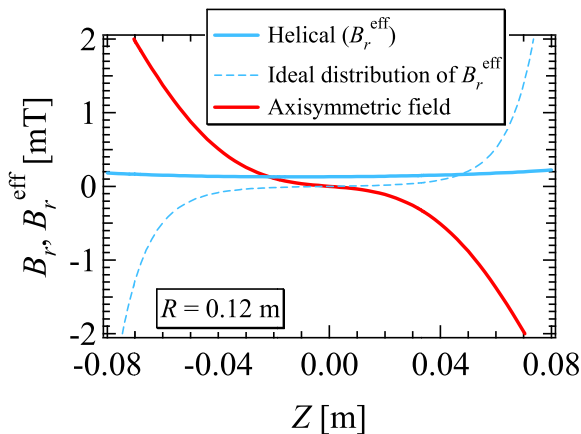


Fig. 10 Radial fields generated by the existing helical coils and the axisymmetric coils as a function of the vertical direction at $R = 0.12$ m.

of the HF coils, the AHF coils, the lower VF coil and the TF coils being 2.6 kAturns, 3.34 kAturns, 0.2 kAturns and 7.5 kAturns, respectively. The radial field generated by the axisymmetric coils was calculated with the currents of the PVF coils, the OH coils, the SC coil and the eddy current being 3.24 kAturns, 1.92 kA, 3.67 kAturns and 10.3 kA, respectively. These coil currents are those at the peak of SC coil current during one of the discharges shown in Fig. 7. The eddy current induced by changes of the PVF coils, the OH coils and the SC coils was calculated by solving the circuit equations where the vacuum vessel was modeled as axisymmetric toroidal conducting elements. The radial field generated by the axisymmetric coils has a vertically antisymmetric distribution ($B_r < 0$ at $Z > 0$, $B_r > 0$ at $Z < 0$), which destabilizes the plasma vertical position. If the effective radial field generated by helical coils has a vertically antisymmetric distribution ($B_r^{\text{eff}} > 0$ at $Z > 0$, $B_r^{\text{eff}} < 0$ at $Z < 0$) like a dotted blue line in Fig. 10, it is expected that it cancels the radial field generated by the axisymmetric coils and then the plasma vertical position is stabilized. However, the effective radial field generated by the existing helical coils is not vertically antisymmetric and

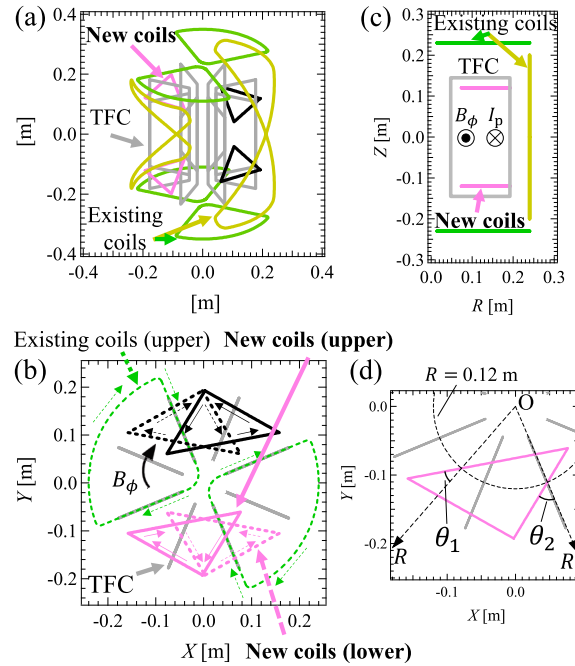


Fig. 11 Design of the new local helical coils. (a) Bird's-eye view, (b) plan view, (c) projection on the poloidal plane, and (d) the enlarged view of (b). The center lines of the coils are shown.

the magnitude is smaller than that generated by the axisymmetric coils, especially at the positions far from the equatorial plane. Thus, the existing local helical coils do not stabilize the plasma vertical position in the experiments.

To improve the effective radial field generated by local helical coils, we designed new local helical coils. Figure 11 shows design of the new local helical coils. Figures 11 (a), (b), (c) and (d) show the bird's-eye view, the plan view, the projection on the poloidal plane and the enlarged view of (b), respectively. The new coils consist of two triangular coils located on upper and lower sides of the plasma inside the TF coils. The coils were named as Upper and Lower Triangular (ULT) coils. The difference from the existing local helical coils, AHF coils, installed on upper and lower sides is that the new coils have parts oblique to, namely neither parallel nor perpendicular to, the radial direction, which generates both radial field and toroidal field. The angles between the parts and the radial direction at $R = 0.12$ m, θ_1 and θ_2 shown in Fig. 11 (d), are $\theta_1 = 38^\circ$ and $\theta_2 = 54^\circ$ in all the ULT coils. The shape of the ULT coils and the values of the θ_1 and θ_2 were determined by the evaluation presented in the next paragraph. Because it is difficult to install a large number of coils in the limited volume inside the TF coils, the number of the ULT coils was determined to be two on both upper and lower sides. The currents of the two coils are opposite to each other.

The shape of the triangular coils was determined to generate the strong effective radial field as possible. Fig-

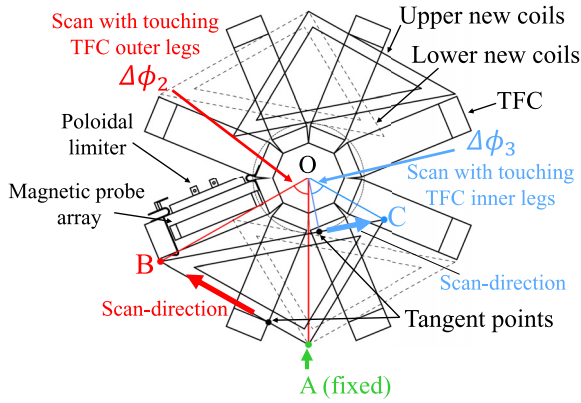


Fig. 12 Schematic view of determining the shape of the triangular coils.

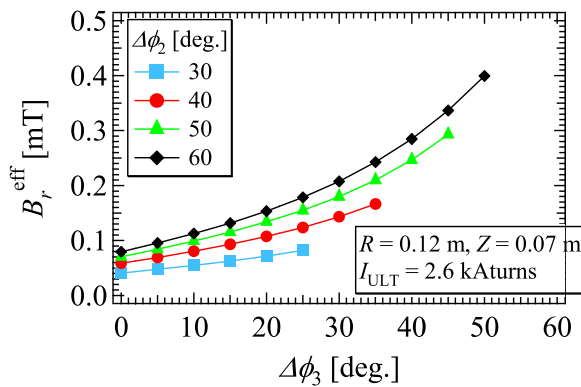


Fig. 13 Effective radial field evaluated in scanning of the shape of the triangular coils in Fig. 12.

ure 12 shows a schematic view showing how we determined the shape of the triangular coils. We fixed one vertex, A, of the upper triangle and put two sides AB and BC so that they touch the legs of the TF coils. The toroidal angle between A and B, $\Delta\phi_2$, and that between the tangent point and C, $\Delta\phi_3$, are scanned within ranges without interference to the other components. The direction of the BC changes depending on $\Delta\phi_2$. The shape of the lower coils is the same as that of the upper coils and the upper and lower coils are installed so that they are symmetrical with respect to OA. The shape of the lower coils is also scanned the same as the upper coils. The range of $\Delta\phi_2$ is limited by the interaction between the outer legs of the TF coils and the upper coils, and that of $\Delta\phi_3$ is limited by the interaction between the support structure of a magnetic probe array and one of the lower coils. We assumed the thickness of the coils was ~ 0.014 m. The center line of the cross-section of the coils was used as a single filament in the magnetic field line calculation. Figure 13 shows the effective radial field evaluated in scanning of the shape of the triangular coils in Fig. 12. The effective radial field is evaluated at $(R, Z) = (0.12 \text{ m}, 0.07 \text{ m})$. The effective radial field increased monotonically with increase in $\Delta\phi_2$ and $\Delta\phi_3$. As a

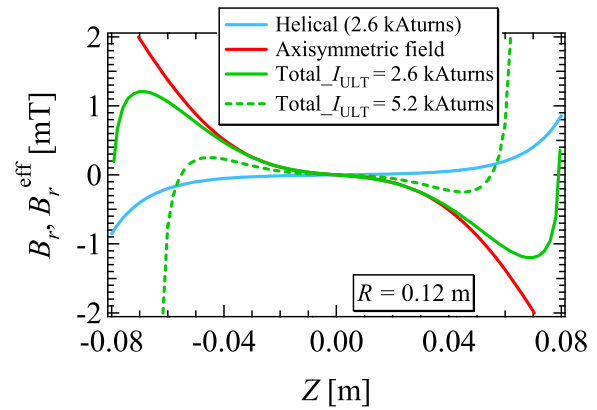


Fig. 14 Radial fields generated by the new helical coils and the axisymmetric coils as a function of the vertical direction at $R = 0.12$ m.

result of Fig. 13, we determined $\Delta\phi_2 = 60^\circ$ and $\Delta\phi_3 = 50^\circ$. In Fig. 11, the center lines of the new coils are drawn using these values. The shape of the triangular coil was determined so that the effective radial field became as strong as possible without interference to the other components.

We calculated the effective radial field using the new local helical coils. The blue line in Fig. 14 shows the effective radial field generated by the new local helical coils as a function of the vertical coordinate Z at $R = 0.12$ m. The currents of ULT coils and TF coils are 2.6 kAturns and 7.5 kAturns, respectively, which are equal to currents of HF coils and TF coils used in Fig. 10. The effective radial field distribution is vertically antisymmetric, and the magnitude becomes stonger rapidly as Z is closer to the upper or lower coil, which is on the same order in comparison to the radial field generated by the axisymmetric coils (red line). The green solid line shows the total radial field generated by combination of the ULT coil current and the axisymmetric coil current. Note that the radial field denoted by the green line does not agree with the sum of those denoted by the blue line and by the red line, because the field line traced in Eq. (1) is different. The effective radial field generated by the ULT coils can reduce the unstable radial field generated by the axisymmetric coils. However, the distribution of the total radial field is still unstable to the plasma vertical position. The green dash line shows the total radial field in the case where the ULT coil current was increased to 5.2 kAturns. The distribution of the radial field becomes almost stable by increasing the ULT coil current. The effective radial field generated by the ULT coils can reduce the unstable radial field generated by the axisymmetric coils as the ULT coil current is increased. Thus, it is expected that the ULT coils can stabilize the plasma vertical position.

We completed the engineering design of the new triangular coils. The number of turns is 60 turns. Figure 15 shows the plan view of the new coils. The corners of the

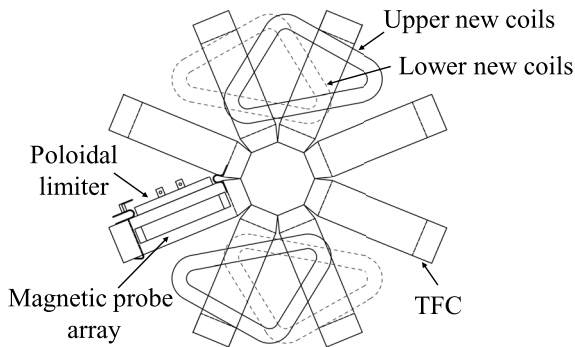


Fig. 15 Plan view of the new local helical coils.

triangle were rounded because it is difficult to wind the wire sharply.

4. Summary

We investigated effects of the helical field generated by the existing local helical coils on the vertical position of the tokamak plasma in TOKASTAR-2. Using the upper and lower axisymmetric coils, SC coils, we generated elongated tokamaks and applied the helical fields. VDEs and plasma current quenches were observed in the case without the helical field. No VDEs were observed when the plasma position was close to the equatorial plane in the case with the small current of the SC coils, while VDEs occurred in any vertical positions in the case with large current of it. This tendency was not improved when the helical field was applied. No suppression of VDEs was observed even though the helical coil currents were increased and the plasma vertical position was adjusted. To investigate

the reason why the helical field was not effective to stabilize the plasma vertical position, we evaluated the effective radial field generated by the helical field. We found that the effective radial field generated by the existing helical coils was not vertically antisymmetric and the magnitude was smaller than that generated by the axisymmetric coils. We therefore concluded that we needed new local helical coils to stabilize the plasma vertical position.

To improve the effective radial field generated by helical coils, we designed triangular coils to be installed on the upper and lower sides of the plasma. The effective radial field generated by the triangular coils can reduce the unstable field which destabilizes the plasma vertical position. We completed the engineering design of the new triangular coils. We will carry out experiments for the stabilization of the plasma vertical position using the new coils.

Acknowledgments

This work is performed with the support and under the auspices of the NIFS Collaboration Research program (NIFS17KLEP026).

- [1] K. Sakurai and S. Tanahashi, *J. Phys. Soc. Jpn* **49**, 759 (1980).
- [2] H. Ikezi, K.F. Schwarzenegger and C. Ludescher, *Phys. Fluids* **22**, 2009 (1979).
- [3] M.C. ArchMiller *et al.*, *Phys. Plasmas* **21**, 056113 (2014).
- [4] A.D. Turnbull *et al.*, *Nucl. Fusion* **56**, 086006 (2016).
- [5] T. Ueda, H. Arimoto, T. Fujita *et al.*, *Plasma Fusion Res.* **10**, 3402065 (2015).
- [6] K. Yasuda, H. Arimoto, A. Okamoto *et al.*, *Plasma Fusion Res.* **13**, 3402072 (2018).
- [7] T. Sakito, H. Arimoto, T. Fujita *et al.*, *Plasma Fusion Res.* **11**, 2402074 (2016).